2013 WJTA-IMCA Conference and Expo
September 9-11, 2013 • Houston, Texas

Paper

EXTENDING ABILITY OF MICRO-HOLE RADIAL HORIZONTAL WELL DRILLED BY HIGH-PRESSURE WATER JET

Chi Huanpeng, Li Gensheng, Huang Zhongwei, Tian Shouceng, Di Fei
State Key Laboratory of Petroleum Resources and Prospecting,
China University of Petroleum-Beijing
Changping, Beijing, China

ABSTRACT

Radial drilling technology with high-pressure water jet, which explores low-permeability and heavy oil reservoirs and the marginal, depleted oil wells effectively and economically, is applied worldwide. Based on hydraulic principles, the pressure loss model of the radial drilling system and the pulling force model of flexible hose connecting with the jet nozzle have been developed. The method to calculate the well extended limit is obtained. A sensitivity study is carried out to identify the parameters controlling the well extended limit. The sensitivity study includes the effect of flow rate, pump pressure, ratio between the flow rate of the forward and backward orifices of the jet nozzle (flow rate ratio for short), well roughness, mother-well depth, and well diameter. The result indicates that the method is reliable to calculate the well extended limit by comparison with result of on-ground test. There exists an optimum flow rate of the forward and backward orifices of the jet nozzle, which is 1.0 in value. The well extended limit is most sensitive to pump pressure, flow rate, well roughness and flow rate ratio. The radial drilling technique is feasible to apply in deep wells. This study can provide theoretical guidance for the multi-orifices nozzle and radial drilling design in field operation.

Organized and Sponsored by WJTA®-IMCA®

1. INTRODUCTION

The radial drilling technique is to drill several micro horizontal wells with diameter of 25-50mm into reservoir at an exact depth perpendicular to the mother-well conveyed by coiled tubing (CT) (Dickinson et al., 1985). It is effective to explore low-permeability or heavy oil reservoirs, and provides a new way to stimulate both live and dead wells with much low cost. The technology has been tested or applied in many countries, such as the USA, Canada, China, Russia, Egypt and some Latin countries (Dickinson et al., 1989; Li Y. H et al., 2000; Stanislav Ursegov et al., 2008; Adel et al., 2011).

The bottom hole assembly (BHA) of radial drilling consists two main parts: a casing milling assembly and a flexible hose connecting with a jet nozzle (**Figure 1**). The operation procedure is simple, that is, after the BHA is anchored at the exact depth in the mother-well, mill a hole on the casing, run in the flexible hose connected with the jet nozzle ahead, and then pumping to drill a drainhole with high-pressure water jet. The jet nozzle is to generate high pressure water jet to break rock and provide the required force to pull the flexible hose forward.

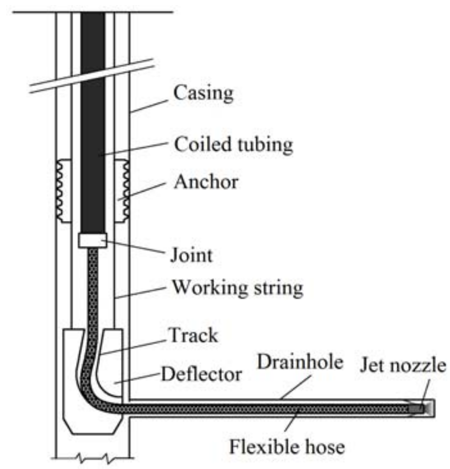

Figure 1. Schematic of radial drilling downhole system

One of the main criteria of radial drilling technology is to drill 4-10 laterals radial from the mother-well, each 1-2in diameter and up to 50m in length (Buset et al., 2001). To create the well as large and long as possible is of great importance, relying on the performance of the jet nozzle. This paper focuses on the method to calculate the well extended limit and how it is been influenced by other parameters.

Buset et al. (2001) studied the penetration mechanism of the jet nozzle and did a preliminary experiment on the pull force which consisted of jetting force, ejector force and under-pressure force. But they didn't carry on studying deeply and their results are not enough to be applied for operation. Guo R. C. et al. (2009) established a model to calculate the pull force of multiple-orifices jet nozzle. But they considered the inlet fluid pressure of the jet nozzle as a positive part for pull force, which is not correct.

The extended limit of the well created by radial drilling hasn't been ever studied theoretically and experimentally. In this paper, the pulling force model is established to calculate the extended limit of the well, and the pressure loss model of the whole radial drilling system to calculate the inlet fluid pressure and the ambient fluid pressure of the jet nozzle. We also carried on a test on ground to validate our method.

2. PULLING FORCE MODEL

By experiment, we find the multiple-orifices jet nozzle is of better performance than other ones in rock-breaking efficiency (Chi H. P. et al. 2013). The major structural parameters are shown in **Figure 2**, including the inner diameter -- d_{in} and outer diameter -- d_{out} of jet nozzle, forward and backward orifice diameters -- d_f and d_b respectively, angle between the orifice axis and jet nozzle axis -- θ_f and θ_b, the inlet angle of orifice -- α, the number of forward and backward orifices – m and n.

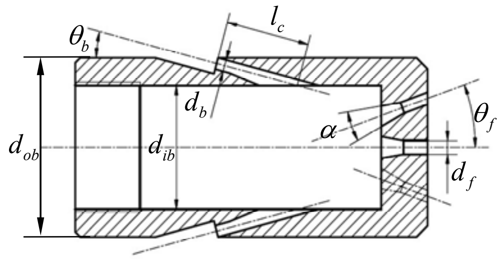

Figure 2. Structure diagram of jet nozzle

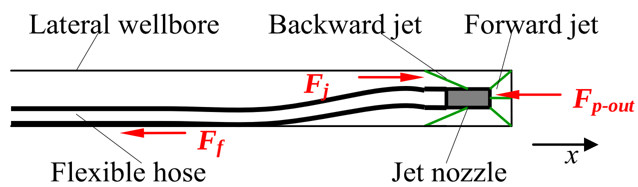

Figure 3. Force analysis of drilling system

As shown in **Figure 3**, during drilling forward by force generated by water jet from orifices on jet nozzle, there are 4 kinds of force on jet nozzle and flexible hose – static ambient fluid pressure on the forward surface of jet nozzle -$F_{p\text{-}out}$, friction force of wellbore and the deflector to flexible hose- F_{df} and F_f respectively, and ejecting force generated by fluid jetting from orifices- F_j. The friction force due to contact between the flexible hose and the deflector is neglected in this study. The pulling force of the flexible hose connected with a jet nozzle ahead is:

$$F_{pull} = F_j - F_{p-out} - F_f \tag{1}$$

where

$$F_{p-out} = \frac{\pi}{4} p_{out} d_{ob}{}^2 \,, \quad F_f = f_d \rho_{hose} g l_{dh} \tag{2}$$

F_{pull} is the resultant force along x-axis direction. When $F_{pull} > 0$, the well is extended forward, the friction - F_f increases at the same time. The F_{pull} will decrease to zero at a certain well length, which is the extended limit of the well and can be calculated by the equation below.

$$l_{EL} = \frac{F_j - F_{p-out}}{f_d \rho_{hose} g} \tag{3}$$

In this equation, to calculate the extended limit- l_{EL}, the ejecting force and ambient fluid pressure should be known first.

Take the fluid within jet nozzle to study (**Figure 4**), and the theorem of momentum is satisfied:

$$\vec{F}t = m\vec{v} \tag{4}$$

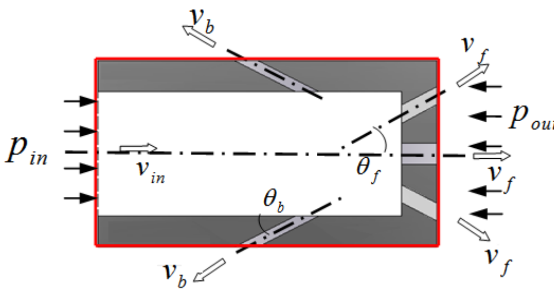

Figure 4. Fluid flowing state within jet nozzle

The forces of the left side in the equation above are generated by the ambient fluid pressure and water jet from orifices. Based on the interaction between the jet nozzle and fluid within which, the following equation can be derived:

$$-F_j + \frac{\pi}{4} p_{out} \left[m d_b^2 \cos\theta_b + (n-1) d_f^2 \cos\theta_f + d_f^2 \right] = \rho Q_f v_f \left[(n-1)\cos\theta_f + 1 \right] - \rho Q_b v_b \cos\theta_b \quad (5)$$

And the p_{out} is the ambient fluid pressure around the jet nozzle. The fluid pressure equals to zero after circulating from the annulus back to the ground, so the p_{out} equals to the pressure loss in the annulus- $p_{a\text{-}loss}$.

The fluid velocity of each orifice can be calculated by the Bernoulli Equation:

$$z_{in} + \frac{p_{in}}{\rho g} + \frac{v_{in}^2}{2g} = z_{out} + \frac{p_{out}}{\rho g} + \frac{v_{out}^2}{2g} + \xi \frac{v_{out}^2}{2g} \quad (6)$$

$$v_j = \sqrt{\frac{2\left(p_{in} - p_{out}\right) + \rho v_{in}^2}{\rho\left(1+\xi\right)}} \quad (7)$$

where ξ is the local resistance coefficient of the orifice (Jamal M. S. 2004).

$$\xi = 0.8 \sin\frac{\alpha}{2}\left(1 - \frac{d_{out}^2}{d_{in}^2}\right) \quad (8)$$

The ratio between the flow rate of the forward and backward orifices of jet nozzle is expressed as:

$$k = \frac{n v_f^2 d_f^2}{m v_b^2 d_b^2} \quad (9)$$

3. PRESSURE LOSS MODEL OF CIRCULATION SYSTEM

To study the inlet fluid pressure and the ambient fluid pressure of the jet nozzle in the model above, the circulation pressure loss should be calculated. The pressure loss of fluid flowing in pipe and annulus can be calculated by equations as follows:

Pipe flow:

$$\Delta p_i = \frac{2f\rho L v^2}{d_i} = 32\frac{f\rho L Q^2}{\pi^2 d_i^5} \tag{10}$$

Annulus flow:

$$\Delta p_a = \frac{2f\rho L v^2}{d_h - d_o} = \frac{32 f\rho L Q^2}{\pi^2 \left(d_h - d_o\right)\left(d_h^{\,2} - d_o^{\,2}\right)} \tag{11}$$

3.1 Pressure Loss of Fluid Flowing in Pipes

The pressure loss of fluid flowing in pipes consists of 3 parts – pressure loss in the spiral section of CT, pressure loss in straight section of CT and pressure loss in the flexible hose.

(1) Pressure loss in the spiral section of CT

Srinivasan P. S. et, al. (1970) derived the friction coefficient of Newtonian fluid flowing in spiral pipe by experiment, as follows:

$$f = \frac{0.084}{N_{\mathrm{Re}}^{\;0.2}}\left(\frac{d}{D}\right)^{0.1} \tag{12}$$

where

$$N_{\mathrm{Re}} = \frac{\rho v d}{\mu} = \frac{\pi \rho Q}{4\mu d} \tag{13}$$

From equation (10), (12) and (13), the analytical equation to calculate the pressure loss in spiral section of CT can be obtained:

$$\Delta p_{ct1} = 0.2596\frac{\mu^{0.2}\rho^{0.8}Q^{1.8}L_{ct1}}{d_{cti}^{4.7}D^{0.1}} \tag{14}$$

To accurately calculate the pressure loss, a field test was carried out. We connected a pressure gage on the inlet of CT and exposed the end of CT to the atmosphere, thus the value of the pressure gage would be the pressure loss of CT. The parameters of tested CT are: outer diameter-0.0254m, inner diameter-0.02m, drum diameter-1.375m, length-4000m. The tested pressure loss is 22MPa. By comparing the experimental result with the value- 24.53MPa calculated by equation (14), the modified equation for equation (14) is:

$$\Delta p_{ct1} = 0.2328\frac{\mu^{0.2}\rho^{0.8}Q^{1.8}L_{ct1}}{d_{cti}^{4.7}D^{0.1}} \tag{15}$$

(2) Pressure loss in the straight section of CT

During radial drilling, the fluid flow in CT or flexible hose is turbulent to guarantee a high impact pressure on formation rock. The friction coefficient during fluid flowing in smooth pipe can be expressed as (F. Gallego et al., 2009):

$$f = \frac{a}{N_{\mathrm{Re}}{}^{b}} \tag{16}$$

where

$$a = \frac{\ln N + 3.93}{50},\ b = \frac{1.75 - \ln N}{7} \tag{17}$$

The radial drilling fluid is water generally, the flow behavior index-N of which is 1.0, and the friction coefficient can be obtained:

$$f = \frac{0.0786}{N_{\mathrm{Re}}{}^{0.25}} \tag{18}$$

Combined equation (18) and (10), we can calculate pressure loss in the straight section of CT by:

$$\Delta p_{ct2} = 0.2399 \rho^{0.75} \mu^{0.25} \frac{L_{ct2}}{d_{cti}^{4.75}} Q^{1.75} \tag{19}$$

(3) Pressure loss in flexible hose

The flexible hose can be studied as straight pipe, and we can use the form of equation (19) to calculate its pressure loss. However, the flexible hose is made of rubber material and CT is a kind of mental tubing. The pressure loss in the flexible hose can not be calculated by equation (19) directly. Thus, we conducted a field test the same as the method to modify equation (14). The results are listed in **Table 1**. The fluid flowing pressure loss per meter can be expressed as:

$$\frac{\Delta p_{hp}}{L_{hp}} = \lambda \rho^{0.75} \mu^{0.25} \frac{1}{d_{hpi}^{4.75}} Q^{1.75} \tag{20}$$

Table 1. Field test results of pressure loss in flexible hose

Length /m	Pressure loss /MPa	Time /s	Weight of water /kg	Flow rate/L· min^{-1}
15	0.8	15.2	11.74	46.46
15	8	7.61	11.53	90.32
15	7	9.18	12.68	82.9
15	5	10.53	12.33	70.26
15	4	12.34	13.55	64.12
22	3.5	15.34	10.98	42.96
22	11.5	8.72	12.73	87.56
22	9	10.18	12.64	74.4
22	5	15.12	13.49	53.96

The relationship between the coefficient- λ and flow rate- Q is shown in **Figure 5**. After linear regression, we obtain the following equation:

$$\lambda = -3.734 \times 10^{-4} Q + 0.494 \tag{21}$$

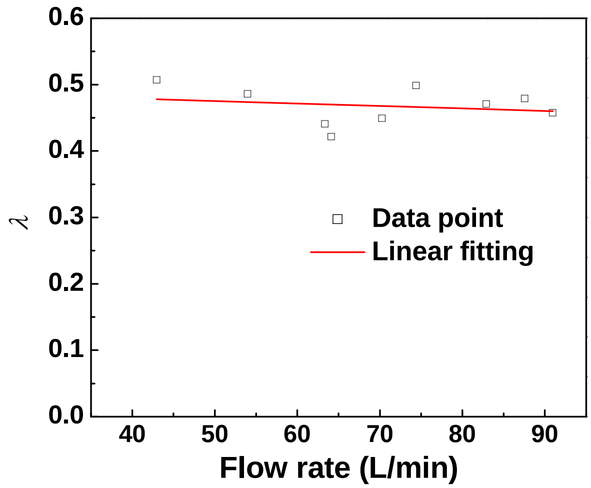

Figure 5. Relationship between flow rate and coefficient-λ

As the flow rate increases, the coefficient- λ changes little. We can take the value- 0.4716 at flow rate- 60L/min as the approximate value of the pressure loss coefficient-λ. Thus, we derive the following equation to calculate the pressure loss in the flexible hose.

$$\Delta p_{hp} = 0.4716 \rho^{0.75} \mu^{0.25} \frac{L_{hp}}{d_{hpi}^{4.75}} Q^{1.75} \tag{22}$$

3.2 Pressure Loss of Fluid Flowing in Annulus

The pressure loss of fluid flowing in annulus consists of two parts -- pressure loss in annulus between wellbore and the flexible hose and pressure loss in annulus between the oil tubing and the vertical wellbore.

Because the open-hole completion is adopted in radial drilling, the roughness of the wellbore must be taken into consideration to calculate the pressure loss in annulus more accurately. The result of Chen (1979) can be used to calculate the friction coefficient of Newtonian fluid flowing in annulus:

$$f = \frac{1}{4}\left\{ \lg\left[\frac{\Delta}{3.7065 d_h} - \frac{5.0452}{N_{\mathrm{Re}}} \lg\left(\frac{1}{2.8257}\left(\frac{\Delta}{d_h}\right)^{1.1098} + \frac{5.8506}{N_{\mathrm{Re}}^{0.8981}} \right) \right] \right\}^{-2} \tag{23}$$

The pressure loss of water flowing in annulus between wellbore and the flexible hose by combining equation (11), (13) and (23) can be derived.

We use equation by Chen T. G et al. (2006) to calculate pressure loss of water flowing in annulus between oil tubing and the vertical wellbore which is much smoother than the horizontal wellbore:

$$\Delta p_{va} = 0.1823 \frac{\rho^{0.8} \mu^{0.2} L_{vw} Q^{1.8}}{\left(d_{vh} - d_{oo}\right)^3 \left(d_{vh} + d_{oo}\right)^{1.8}} \tag{24}$$

4. SENSITIVITY STUDY

Based on the method established above and the parameters of jet nozzle in **Table 2**, a sensitivity study is carried out to identify the parameters controlling the well extended limit. The sensitivity study includes the effect of flow rate, pump pressure, ratio between the flow rate of the forward and backward orifices of the jet nozzle (flow rate ratio for short), well roughness, mother-well depth, and well diameter.

Table 2. Structural parameters of jet nozzle

Parameter	Value	Parameter	Value
forward orifice diameter /mm	0.5	backward orifice diameter /mm	0.262
angle between forward orifice axis and jet nozzle axis /rad	0.524	angle between backward orifice axis and jet nozzle axis /rad	15
the number of forward orifices	6	the number of backward orifices	8
inner diameter /mm	10	outer diameter /mm	18
inlet angle of the orifice /rad	0.236		

4.1 Effect of the Flow Rate

The extended limit of the well decreases along with the increase of flow rate (**Figure 6**). To make the well extend longer, a lower flow rate should be selected. But the rock-breaking efficiency is low with a lower flow rate. There is an optimum value of flow rate -- 60L/min to balance the well extension and rock-breaking efficiency combining with the research of Liao H. L. et al. (2012).

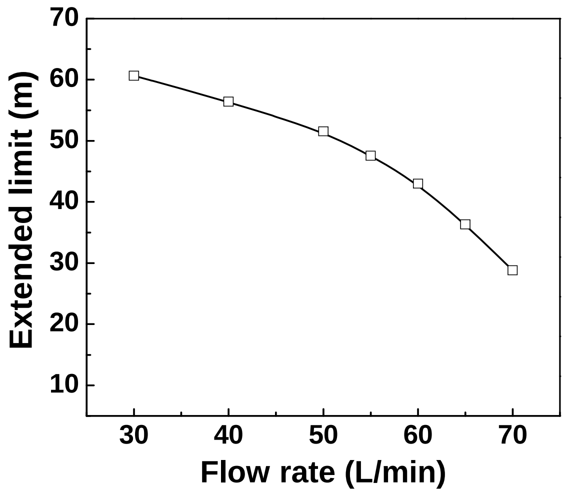

Figure 6. Relationship between flow rate and extended limit of horizontal well

4.2 Effect of the Pump Pressure

Figure 7 illustrates how the extended limit changes with the change in pump pressure from 30MPa to 60MPa. Pump pressure can increase the well extended limit significantly because of the increasing inlet fluid pressure of the jet nozzle. Then, to increase the pump pressure is recommended if the operation equipment and security condition allow in field operation.

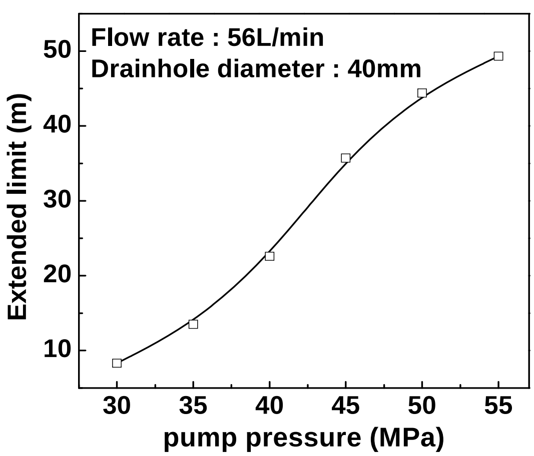

Figure 7. Effect of pump pressure

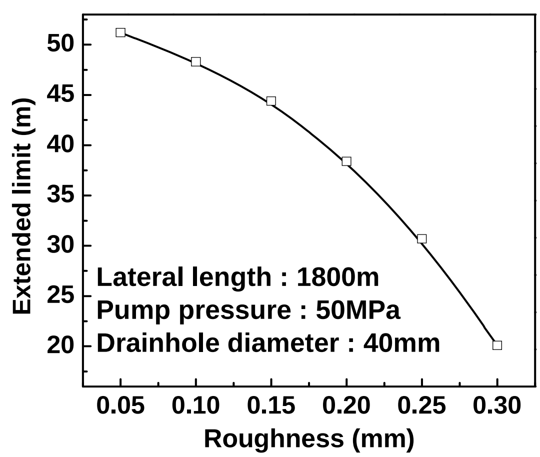

Figure 8. Effect of well roughness

4.3 Effect of the Well Roughness

The roughness of the well has an important effect on both annulus pressure loss and pressure drawdown during production. In **Figure 8**, the well extended limit decreases with a more and more high speed, that is because both the friction force on the flexible hose and the ambient pressure around the jet nozzle increase as the roughness increases. Thus, the ejecting force decreases, resulting in the decrease of well extended limit.

4.4 Effect of the Flow Rate Ratio

The well extended limit can change a lot when the flow rate ratio- k changes by changing the ejecting force of the jet nozzle at the same pumping flow rate. The well extended limit of the ideal condition (nozzle discharge coefficient = 1.0) and the actual condition (nozzle discharge coefficient = 0.7-0.8) for different flow rate ratios are shown in **Figure 9**. The semi-log plots in the figure are like downward parabola. The optimum flow rate ratio is about 1.0. And the extended limit of ideal condition is about two times as that of actual condition. Improving the nozzle discharge coefficient can help to extend the well length.

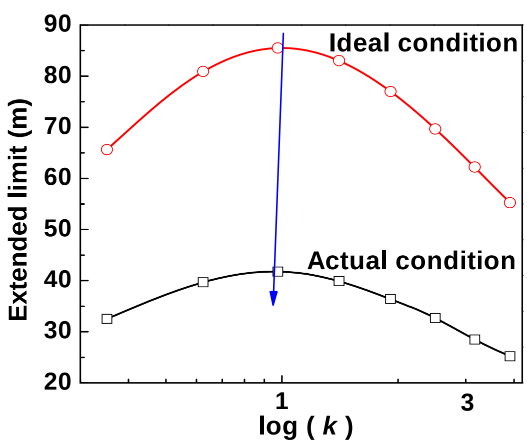

Figure 9. The effect of flow rate ratio

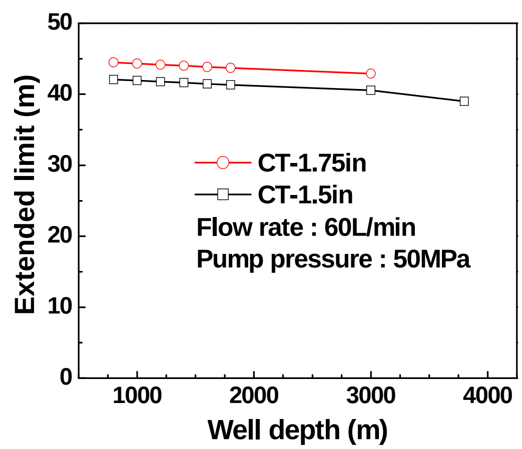

Figure 10. The effect of mother-well depth

4.5 Effect of Mother-Well Depth

The radial drilling is generally applied in shallow wells, and seldom is the application in deep wells reported except in Bolivia reported by Raúl Andrés Cirigliano (2007). The influence of mother-well depth on the well extended depth for two kinds of CT are shown in **Figure 10**. The extended limit of 1.75in CT is a bit larger than that of 1.5in CT because of less pressure loss in CT. The plots are nearly parallel to the abscissa axis and there is only two meters' decease from mother-well depth 800m to 3800m, indicating that the effect of mother-well depth on the well extended limit is negligible.

4.6 Effect of the Well Diameter

The well extended limit increases by increasing the well diameter, but the increasing speed decreases as shown in **Figure 11**. That is because small well diameter will result in large pressure loss in well annulus and large resistance from ambient fluid around the jet nozzle.

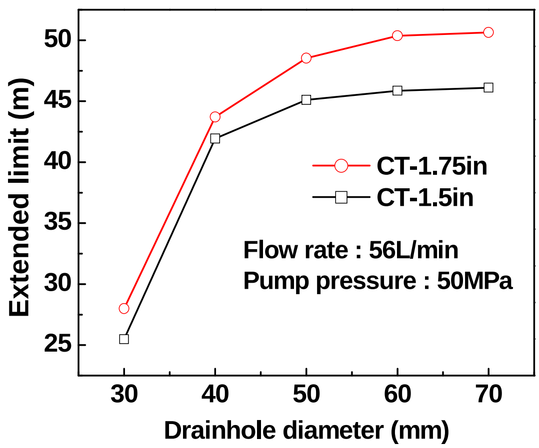

Figure 11. The effect of well diameter

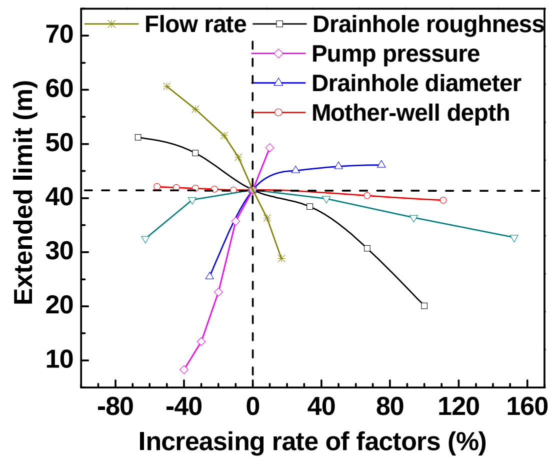

Figure 12. Sensitivity analysis

4.7 Sensitivity Analysis

By sensitivity analysis method, we quantify the level that how changes in the different parameters above impact the extended limit of the well. The relationship of the dimensionless changing rate of the four parameters and the well extended limit is shown in **Figure 12**. The pump pressure, flow rate, well roughness and flow rate ratio of jet nozzle are dominant parameters that influence the extended limit, which indicates that the pumping capacity and jet nozzle performance are of great importance to radial drilling technique. Meanwhile, the extended limit is not sensitive to changing of the mother-well depth, revealing that the radial drilling technique is feasible in deep wells.

5. GROUND TEST

To validate the models developed above, as well as to examine the reliability of the downhole tools, a test was carried out on ground. The porous concrete blocks with 0.6 meter long, 0.24 meter wide and 0.12 meter high of each, were adopted as formation rocks. These blocks were tied up and placed parallel to the ground with downhole tools, as showing in **Figure 13**. The major parameters of the other equipment and tools are listed in **Table 3**.

Table 3. Major ground test parameters

Coiled tubing		Flexible hose		Pump pressure / MPa	Flow rate / $L \cdot min^{-1}$
Length /m	Inner diameter /mm	Length /m	Inner diameter /mm		
30	32	22	10	30	70

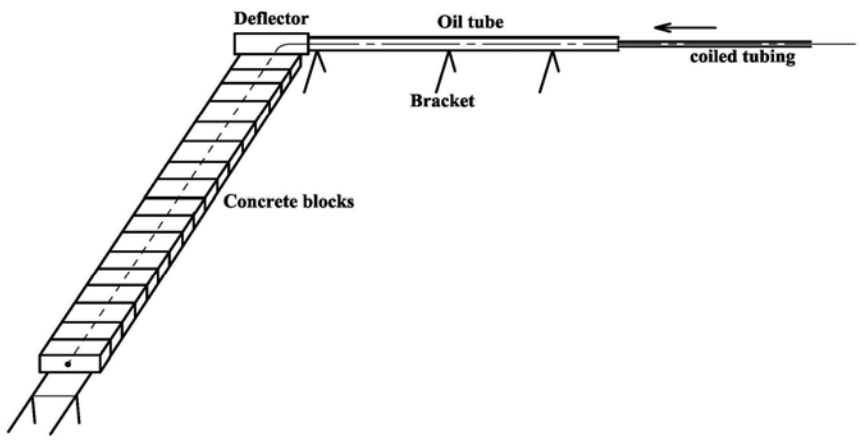

Figure 13. Schematic of ground test of hydra-jet radial drilling

86 blocks were drilled out with a total length 20.64 meters and 27mm in hole diameter (**Figure 14**). The extended limit calculated by our models is 24.37m based on the test parameters, with a relative error – 18% compared with the test result. This is mainly because the friction of deflector to flexible hose is larger in test condition than that in theory. However, the relative error is acceptable. And we can conclude that the method we have developed can provide reliable prediction of well extended limit by high-pressure water jet.

Figure 14. Results of ground test

6. CONCLUSIONS

(1) The equation to calculate pressure loss in the spiral section of CT is modified by field test. And the pressure loss equation in flexible hose is established.
(2) The optimum flow rate is 60L/min balancing the well extension and rock-breaking efficiency. The well extended limit increases as the pump pressure increases. The larger and smoother the well is, the longer the well extends. There is an optimum value of the ratio between the flow rate of the forward and backward orifices of the jet nozzle, which is about 1.0 in this study.
(3) The pump pressure, flow rate, well roughness and flow rate ratio of jet nozzle are dominant parameters that influence the well extended limit. The feasibility of application of radial drilling technology in deep wells is proved theoretically.
(4) The extended limit of calculated outcome is 18% larger than that of the ground test. The models and method we develop can provide reliable prediction of well extended limit by high-pressure water jet.

ACKNOWLEDGEMENTS

The authors express their appreciation to the National Basic Research Program of China (2010CB226700), the Major International Joint Research Project of National Natural Science Foundation of China (51210006) and Major National Science and Technology Program of China (2011ZX05036-002) for their supports for this work.

RERFERENCES

W. Dickinson, R. W. Dickinson, (1985) Horizontal Radial Drilling System, *SPE California Regional Meeting*, SPE 13949.

W. Dickinson, R. R. Anderson, R. W. Dickinson, (1989) The Ultrashort-Radius Radial System, *SPE Drilling Engineering*, 4(3), 247-254.

Li Y. H, Wang C. J, Shi L. H, (2000) Application and Development of Drilling and Completion of the Ultrashort-Radius Radial Well by High Pressure Jet Flow Techniques, *The China International Oil and Gas Conference and Exhibition*, SPE 64756.

Stanislav Ursegov, Alexander Bazylev and Evgeny Taraskin, (2008) First Results of Cyclic Steam Stimulations of Vertical Wells with Radial Horizontal Bores in Heavy Oil Carbonates, *The Russian Oil and Gas Technical Conference and Exhibition*, SPE 115125.

P. Buset and M. Riiber, (2001) Jet Drilling Tool: Cost-Effective Lateral Drilling Technology for Enhanced Oil Recovery, *SPE/ICoTA Coiled Tubing Roundtable*, SPE 68504.

Guo R. C., Li G. S. and Huang Z. W. et al., (2009) Experiment Study and Theoretical Analysis of Pulling Force of Self-feeding Hydraulic Bit, *Petroleum Science*, 4, 395-399.

Chi H. P.. Li G. S. and Liao H. L. et al., (2013) Experimental Research on Optimum of Jet Bit in Radial Drilling by Hydra-jet, *Fluid Machinery*, 41(2), 1-6.

Jamal M. S., (2004) *Fluid Flow Handbook - Chinese Edition*, Beijing: Sinopec Press, 139-158.

P. S. Srinivasan, S. S. Nandapurkar and F. A. Holland, (1970) Friction Factors for Coils, *Transactions of the Institution of Chemical Engineers*, 48(1), 156-161.

F. Gallego, S. N. Shah, (2009) Friction Pressure Correlations for Turbulent Flow of Drag Reducing Polymer Solutions in Straight and Coiled Tubing, *Journal of Petroleum Science and Engineering*, 65(3/4), 147-161.

Chen N. H., (1979) An Explicit Equation for Friction Factor in Pipe, *Ind. Eng. Chem. Fundam.,* 18(3), 296-297.

Chen T. G., Guan Z. C., (2006) *Theory and Technology of Drilling Engineering*, Dongying: China University of Petroleum Press, 148-154.

Raúl Andrés Cirigliano, Juan Felipe Talavera Blacutt, (2007) First Experience in the Application of Radial Perforation Technology in Deep Wells, *Latin American & Caribbean Petroleum Engineering Conference,* SPE 107182.

Liao H. L., Li G. S., et al., (2011) Experiment Study on Water Jet Breaking Rock by Multi-orifice Nozzle, *Journal of China Coal Society*, 36(11), 1858-1862.

NOMENCLATURE

d_b = backward nozzle diameter of the jet bit, m
d_{cti} = inner diameter of CT, m
d_f = forward nozzle diameter of the jet bit, m
d_h = wellbore diameter, m
d_{hp} = inner diameter of high-pressure hose, m
d_{in} = inner diameter of the jet bit, m
d_o = outer diameter of the pipe, m
d_{oo} = outer diameter of oil tubing, m
d_{out} = nozzle diameter, m
d_{vh} = diameter of vertical wellbore, m
D = drum diameter of CT, m
f = hydraulic friction coefficient, dimensionless
f_d = well friction coefficient, dimensionless
$F_{p\text{-}out}$ = static ambient fluid pressure on forward surface of the jet bit, N
F_f = friction force of well to high-pressure hose, N
F_j = ejecting force generated by fluid jetting from nozzles, N
F_{pull} = pulling force of the high-pressure hose and the jet bit, N
g = gravitational acceleration, 9.8m/s^2
k = ratio between the flow rate of the forward and backward nozzles (flow rate ratio for short), dimensionless
l_{EL} = well extended limit, m
L = pipe length, m
L_{ct1} = length of the spiral section of CT, m

L_{ct2} = length of the straight section of CT, m
L_{hp} = length of the high-pressure hose, m
L_{vh} = length of the vertical wellbore, m
m = the number of backward nozzles of the jet bit, dimensionless
n = the number of forward nozzles of the jet bit, dimensionless
N = flow behavior index, dimensionless
N_{Re} = Renold number, dimensionless
$p_{a\text{-}loss}$ = pressure loss in the annulus, Pa
p_{in} = inlet fluid pressure of the jet bit, Pa
p_{out} = ambient fluid pressure around the jet bit, Pa
p_r = rated pump pressure, MPa
P_r = rated power of the pump, kW
Q = flow rate, m^3/s
Q_r =rated flow rate of the pump, L/s
v = fluid velocity with pipe, m/s
v_b = jet velocity from the backward nozzle, m/s
v_f = jet velocity from the forward nozzle, m/s
v_{in} = inlet fluid velocity of the jet bit, m/s
v_{out} = jet velocity from the nozzle, m/s
Δ = roughness of well, m
Δp_i = pressure loss in pipe, Pa
Δp_a = pressure loss in annulus, Pa
Δp_{ct1} = pressure loss in spiral section of CT, Pa
Δp_{ct2} = pressure loss in straight section of CT, Pa
Δp_{hp} = pressure loss in high-pressure hose, Pa
Δp_{va} = pressure loss in vertical annulus, Pa
α = inlet angle of the nozzle, rad
θ_f = angle between the forward nozzle axis and the jet bit axis, rad
θ_b = angle between the backward nozzle axis and the jet bit axis, rad
λ = pressure loss coefficient in high-pressure hose, dimensionless
μ = viscosity of water, Pa·s
ρ = density of water, kg/m^3
ρ_{hose} = weight of high-pressure hose per meter, kg/m
ξ = local resistance coefficient of the nozzle, dimensionless